genesis 46:546–552 (2008)

TECHNOLOGY REPORT

Generation of a Conditional Null Allele for *Cftr* in Mice

Craig A. Hodges,[1] Calvin U. Cotton,[1,2] Mark R. Palmert,[3] and Mitchell L. Drumm[1,4]*

[1]Department of Pediatrics, Case Western Reserve University School of Medicine, Cleveland, Ohio
[2]Department of Physiology and Biophysics, Case Western Reserve University School of Medicine, Cleveland, Ohio
[3]Department of Pediatrics, Division of Endocrinology, The Hospital for Sick Children, The University of Toronto, Ontario, Canada
[4]Department of Genetics, Case Western Reserve University School of Medicine, Cleveland, Ohio

Received 8 May 2008; Revised 22 July 2008; Accepted 2 August 2008

Summary: The cystic fibrosis transmembrane conductance regulator (*CFTR*) gene encodes a cAMP-regulated chloride channel that is important in controlling the exchange of fluid and electrolytes across epithelial cells. Mutation of *CFTR* can lead to cystic fibrosis (CF), the most common lethal genetic disease in Caucasians. CF is a systemic illness with multiple organ systems affected including pulmonary, gastrointestinal, pancreatic, immune, endocrine, and reproductive systems. To understand the role of CFTR in the various tissues in which it is expressed, we generated a murine conditional null allele of *Cftr* (*Cftr*^{fl10}) in which *loxP* sites were inserted around exon 10 of the *Cftr* gene. The *Cftr*^{fl10} allele was validated by generating constitutive *Cftr* null (*Cftr*$^{\Delta 10}$) mice using the protamine-cre system. The *Cftr*$^{\Delta 10/\Delta 10}$ mice displayed almost identical phenotypes to previously published CF mouse models, including poor growth, decreased survival, intestinal obstruction, and loss of Cftr function as assessed by electrophysiology measurements on gut and nasal epithelium. Mice containing the conditional null *Cftr* allele will be useful in future studies to understand the role of Cftr in specific tissues and developmental time points and lead to a better understanding of CF disease. genesis 46:546–552, 2008. **© 2008 Wiley-Liss, Inc.**

Key words: Cftr; cystic fibrosis; mouse model; conditional knockout; ion transport; intestinal obstruction

Mutation of the cystic fibrosis transmembrane conductance regulator (*CFTR*) gene can lead to cystic fibrosis (CF), an autosomal recessive disorder which occurs in about 1 in every 3,000 Caucasian live births. The CFTR protein is a chloride channel involved in the exchange of fluid and electrolytes across epithelial cells (Gadsby *et al*., 2006). CF is a systemic disorder consistently characterized by poor growth, chronic lung infection, exocrine pancreatic insufficiency, intestinal malabsorption, reduced fertility, and shortened lifespan. Many patients with CF experience meconium ileus, distal intestinal obstructive syndrome, delayed puberty, liver disease, and diabetes. Although these phenotypes ultimately arise as a consequence of reduced or absent CFTR function, the wide expression of *CFTR* throughout the body makes it difficult to establish the mechanism behind the variety of phenotypes. For example, poor growth may be due to loss of CFTR in the intestinal tract, pancreas, neuroendocrine cells, or any combination thereof. *CFTR* is expressed in many epithelial tissues such as lung (Engelhardt *et al*., 1992; Trezise and Buchwald, 1991; Trezise *et al*., 1993a), nose (Engelhardt *et al*., 1992), salivary glands (Manson *et al*., 1997; Trezise and Buchwald, 1991), intestine (Manson *et al*., 1997; Trezise and Buchwald, 1991), stomach (Manson *et al*., 1997), pancreas (Trezise and Buchwald, 1991; Trezise *et al*., 1993a), liver (Yang *et al*., 1993), gall bladder (Yang *et al*., 1993), sweat gland (Kartner *et al*., 1992), kidney (Todd-Turla *et al*., 1996), male and female reproductive tracts (Trezise *et al*., 1993a,b), thyroid (Devuyst *et al*., 1997) and the early embryo (Ben-Chetrit *et al*., 2002) as well as nonepithelial tissues such as heart (Davies *et al*., 2004), brain (Mulberg *et al*., 1998), smooth muscle (Robert *et al*., 2004) and lymphocytes (Yoshimura *et al*., 1991). The identification of *CFTR*'s role in each of these tissues will facilitate the understanding of CF disease.

Currently available mouse models of CF were created using conventional gene targeting strategies leading to constitutive null or hypomorphic alleles of *Cftr*. While the lung pathology so prevalent in human CF patients is mostly absent in these mouse models, Cftr-deficient mice do display multiple CF phenotypes including poor growth, intestinal obstruction, delayed puberty, infertility, pancreatic abnormalities, gall bladder abnormalities, and decreased survival (Colledge *et al*., 1995; Delaney *et al*., 1996; Grubb and Boucher, 1999; Hasty *et al*., 1995; Hodges *et al*., 2008; Jin *et al*., 2006; Kent *et al*., 1996; O'Neal *et al*., 1993; Ratcliff *et al*., 1993; Rozmahel

*Correspondence to: Dr. Mitchell Drumm, Department of Pediatrics, Case Western Reserve University School of Medicine, Cleveland, OH 44106, USA. E-mail: mitchell.drumm@case.edu.

Published online 18 September 2008 in Wiley InterScience (www.interscience.wiley.com).
DOI: 10.1002/dvg.20433

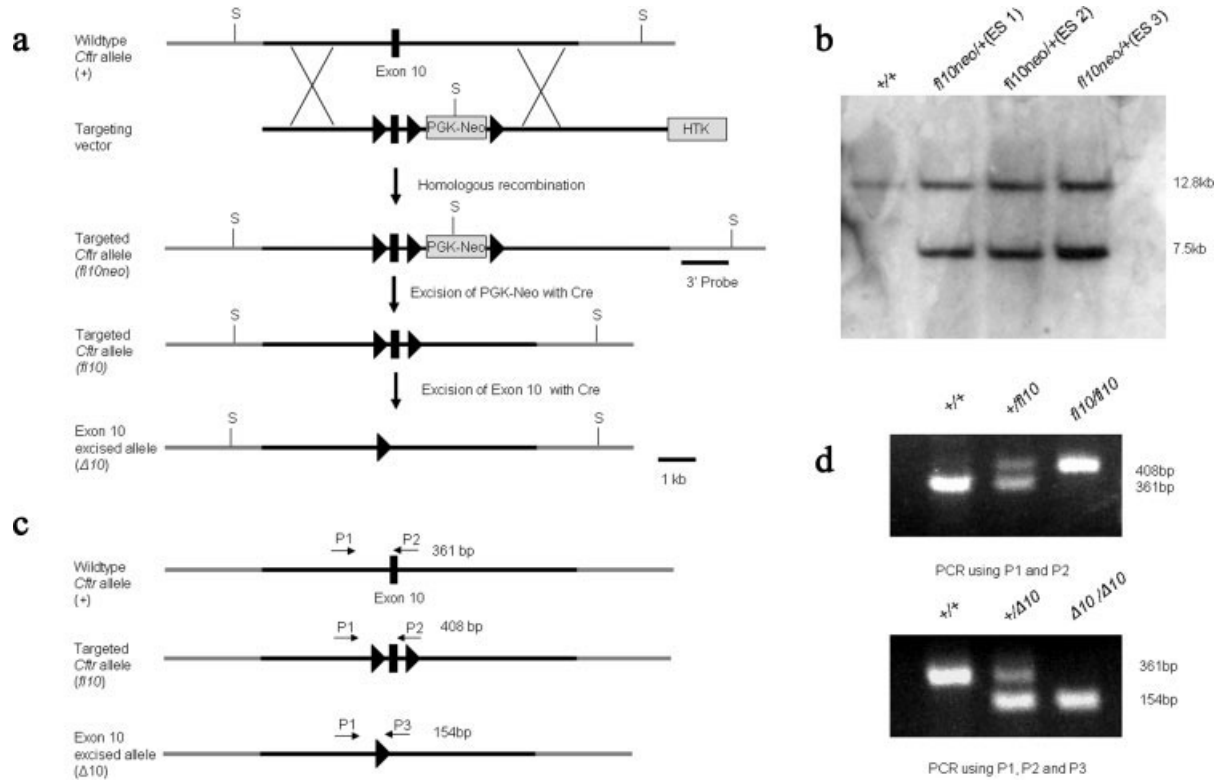

FIG. 1. Generation of the *Cftr* conditional null allele. (**a**) The wild-type *Cftr* allele contains exon 10 of *Cftr* (black box). The targeting vector contains three *loxP* sites (triangles) that flank both exon 10 and the PGK-Neo. Both arms of the targeting vector have ~4.5-kb homologous sequence to Cftr. A HTK-selectable marker was also included for negative selection. A 3′ probe was used in conjunction with Sph1 restriction enzyme (S) to detect correct targeting events by Southern blotting ($Cftr^{fl10neo}$). Recombination of the *loxP* sites surrounding PGK-Neo results in a floxed exon 10 of *Cftr* ($Cftr^{fl10}$) without PGK-Neo. Recombination of the remaining *loxP* sites results in the excision of exon 10 leaving one *loxP* site ($Cftr^{\Delta 10}$). (**b**) Southern blot analysis of three correctly targeted ES cell lines along with the wild-type R1 cell line. Correctly targeted ES cells displayed a unique 7.5-kb band when compared with wild-type cells. (**c**) PCR strategy for detecting the conditional null allele. P1 and P2 amplify 361- and 408-bp fragments from the wild-type ($Cftr^{+}$) and conditional null allele ($Cftr^{fl10}$) respectively. P1 and P3 amplify a 154-bp fragment from the exon 10 deleted allele ($Cftr^{\Delta 10}$). (**d**) A representative agarose gel image of the PCR results.

et al., 1996; Snouwaert *et al*., 1992; Zeiher *et al*., 1995). As in the human, it is not clear how the etiology of these phenotypes relate to each other, because in these global knockouts, the physiology of the tissues involved overlap. Thus, fully understanding the effects of losing Cftr in individual tissues or organs of the mouse cannot be accomplished through conventional gene knockout approach.

To better understand the physiologic relationship of CF-affected tissues and organs, we created a conditional null *Cftr* allele in the mouse. Here we describe the generation of a murine *Cftr* allele with *loxP* sites flanking exon 10 allowing conditional deletion of exon 10 by directed expression of the bacterial Cre recombinase. Exon 10 of *Cftr* was chosen as a target because of its known importance in protein function. Not only are many exon 10 mutations associated with CF in humans (Tsui, 1992) but also the disruption of exon 10 in mice is known to create severe CF phenotypes (Colledge *et al*., 1995; Ratcliff *et al*., 1993; Snouwaert *et al*., 1992; Zeiher *et al*., 1995). In addition, future comparison of this model with other null or hypmorphic *Cftr* alleles of exon 10 should be straightforward because the same region of the gene is altered in other *Cftr* mouse models.

The mouse *Cftr* gene consists of 27 exons and spans over 150 kb. To generate a conditional null allele of *Cftr*, we constructed a targeting vector in which exon 10 of the *Cftr* gene was flanked by *loxP* sites (see Fig. 1), or "floxed". The vector also contained selectable markers for both positive (neomycin resistance cassette) and negative (herpes thymidine kinase gene, HTK) selection of mouse embryonic stem (ES) cells. The neomycin cassette was surrounded by *loxP* sites allowing for its removal with Cre recombinase expression as well. R1 ES cells were electroporated with the targeting vector and neomycin resistant colonies were used for DNA blot confirmation of correct targeting of the 3′ end of the construct (see Fig. 1). Three ES colonies out of 201(1.5%) tested were correctly targeted. Additional PCR strategies were used to confirm correct homologous recombination on both the 5′ and 3′ ends (data not shown). Chimeras were generated from two of the correctly targeted ES colonies using standard procedures. Germline transmission of the conditional null allele of *Cftr* ($Cftr^{fl10neo}$) was confirmed by both Southern blotting and PCR analysis

(see Fig. 1). The neomycin cassette was removed in subsequent generations of mice (referred to as $Cftr^{fl10}$) using Cre recombinase to circumvent any possible complications caused by the presence of the neomycin cassette. Mice homozygous for the conditional null allele ($Cftr^{fl10/fl10}$) were indistinguishable from wild-type mice in growth, survival, and Cftr activity.

To validate the utility of our conditional null *Cftr* allele, we generated a constitutive deletion of exon 10 by crossing mice with the $Cftr^{fl10}$ allele to mice expressing Cre recombinase during the final stages of spermatogenesis through a protamine promoter (O'Gorman *et al.*, 1997). Male mice heterozygous for the $Cftr^{fl10}$ allele and positive for protamine Cre recombinase were mated to wild-type females resulting in a portion of offspring heterozygous for a deleted exon 10 allele ($Cftr^{\Delta 10/+}$). The $Cftr^{\Delta 10/+}$ mice were mated to generate $Cftr^{\Delta 10/\Delta 10}$ mice which were verified by PCR analysis (see Fig. 1). The transmission of the $Cftr^{\Delta 10}$ allele followed Mendelian inheritance proportions with 22 (24.4%) wild-type $Cftr^{+/+}$, 46 (51.1%) heterozygote $Cftr^{\Delta 10/+}$, and 22 (24.4%) homozygote mutant mice $Cftr^{\Delta 10/\Delta 10}$.

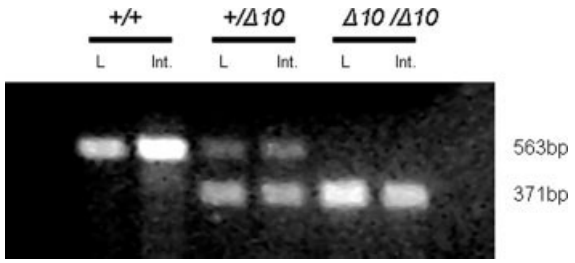

FIG. 2. Expression of *Cftr* in $Cftr^{+/+}$, $Cftr^{+/\Delta 10}$, and $Cftr^{\Delta 10/\Delta 10}$ mice. Amplification of exons 8–11 from cDNA created from RNA from lung (L) and intestine (Int.) display a 563-bp product from the wild-type allele and a 371-bp product from the exon 10 deleted allele (the 192-bp exon 10 is absent in the $Cftr^{\Delta 10}$ allele).

The removal of exon 10 in *Cftr* creates an in-frame deletion in which *Cftr* is transcribed but exon 10 is absent from the RNA (see Fig. 2). Antibodies raised to Cftr will not distinguish between Cftr containing and lacking exon 10 and so functional assays were employed to determine the effects of the allele. To test for Cftr function, we assayed Cftr's ability to conduct chloride across the nasal and intestinal epithelium in $Cftr^{fl10/fl10}$, $Cftr^{+/+}$, and $Cftr^{\Delta 10/\Delta 10}$ mice. Nasal potential difference (NPD) across the nasal epithelium was measured before and after the addition of a chloride-free solution containing forskolin (Fig. 3a). Forskolin stimulates adenylate cyclase, leading to activation of Cftr through protein kinase A-mediated phosphorylation. Challenge with a nominally chloride-free solution provides a concentration gradient in favor of chloride secretion. NonCF animals display chloride secretion in response to this challenge, generat-

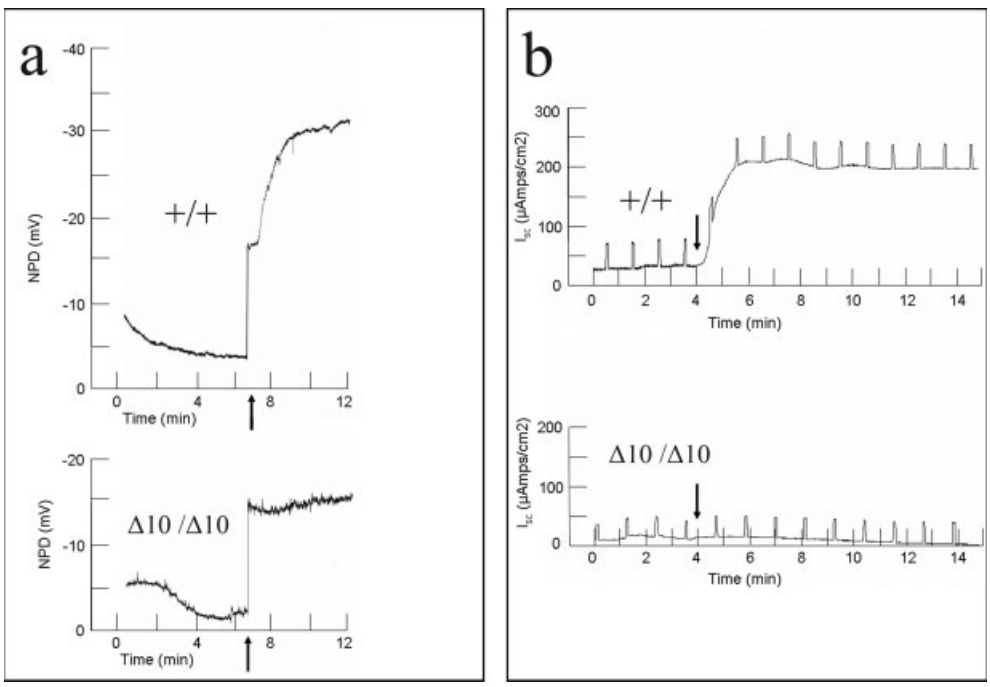

FIG. 3. Electrophysiology in $Cftr^{+/+}$ and $Cftr^{\Delta 10/\Delta 10}$ mice. (**a**) NPD of $Cftr^{+/+}$ and $Cftr^{\Delta 10/\Delta 10}$ mice. Arrow indicates the addition of forskolin (10 μM) and chloride-free HEPES-buffered Ringer's solution. A bi-ionic junction potential of −13 mV was observed (step increase in voltage coincident with solution change) independent of mouse genotype and was excluded from the calculation of change in NPD. (**b**) Intestinal short-circuit current in $Cftr^{+/+}$ and $Cftr^{\Delta 10/\Delta 10}$ mice. Arrow indicates the addition of forskolin (10 μM) and IBMX (100 μM). Vertical deflections (at 1-min intervals) result from voltage-clamp to non-zero values to measure transepithelial resistance. ($Cftr^{fl10/fl10}$ mice were indistinguishable from $Cftr^{+/+}$ mice).

ing a lumen-negative potential difference, while CF mice do not respond (Fig. 3a). After solution perfusion, $Cftr^{fl10/fl10}$ animals showed a change in NPD of -15.8 ± 5.2 mV, $Cftr^{+/+}$ animals showed a change in NPD of -25.0 ± 6.8 mV, while $Cftr^{\Delta 10/\Delta 10}$ animals showed a change of only -0.5 ± 0.5 mV ($P < 0.01$ for $Cftr^{\Delta 10/\Delta 10}$ vs. either control group; three mice per genotype). The lack of change in NPD in $Cftr^{\Delta 10/\Delta 10}$ mice is consistent with absence of Cftr activity.

Cftr function in the intestinal epithelium was assessed by measuring short-circuit current across intestinal sections before and after stimulation by a cocktail of forskolin and IBMX to raise cAMP levels. This maneuver increases short-circuit current in nonCF animals but not in CF animals (Fig. 3b). Intestinal sections from the ileum, jejunum, duodenum, cecum, and colon were tested for change in short-circuit current and all showed similar differences between $Cftr^{fl10/fl10}$, $Cftr^{+/+}$, and $Cftr^{\Delta 10/\Delta 10}$ animals (Table 1). The lack of increase in short-circuit current in $Cftr^{\Delta 10/\Delta 10}$ mice is consistent with the absence of Cftr function in the intestinal epithelium.

Table 1
Effect of Forskolin/IBMX on Short-Circuit Current Across Intestinal Epithelium

Intestinal tissue	$Cftr^{fl10/fl10}$ ΔI_{sc} ($\mu A/cm^2$)[a]	$Cftr^{+/+}$ ΔI_{sc} ($\mu A/cm^2$)	$Cftr^{\Delta 10/\Delta 10}$ ΔI_{sc} ($\mu A/cm^2$)
Duodenum	87.81 ± 20.6	153.66 ± 24.6	1.10 ± 1.0*
Jejunum	92.17 ± 27.8	121.61 ± 22.6	3.47 ± 1.5*
Ileum	98.90 ± 24.8	238.25 ± 24.4	2.15 ± 1.8*
Cecum	155.16 ± 37.4	291.57 ± 77.6	0.49 ± 0.2*
Colon	131.00 ± 42.7	129.49 ± 19.1	0.32 ± 0.4*

[a] ΔI_{sc} ($\mu A/cm^2$) is averaged from a minimum of four measurements per tissue and five mice per genotype; mean ± SE.
*$P < 0.05$ vs. $Cftr^{fl10/fl10}$ or $Cftr^{+/+}$.

The $Cftr^{\Delta 10/\Delta 10}$ mice displayed decreased growth and decreased survival (see Fig. 4) similar to other published reports of CF mouse models (Colledge *et al*., 1995; Delaney *et al*., 1996; Hasty *et al*., 1995; O'Neal *et al*., 1993; Ratcliff *et al*., 1993; Rozmahel *et al*., 1996; Snouwaert *et al*., 1992; Zeiher *et al*., 1995). Growth was reduced in $Cftr^{\Delta 10/\Delta 10}$ mice by an average of 17%–39% depending on the age of the animals (see Fig. 4) similar to the 20%–50% growth reduction observed in *Cftr* null models. The $Cftr^{\Delta 10/\Delta 10}$ mice also displayed decreased survival compared with littermates with only 32% surviving up to 40 days similar to the 5%–40% survival observed in *Cftr* null models. The majority of deaths in $Cftr^{\Delta 10/\Delta 10}$ mice occurred shortly after weaning (20–30 days) due to intestinal obstruction (Figs. 4c and 5). Further examination of the intestine of $Cftr^{\Delta 10/\Delta 10}$ mice revealed typical intestinal histology observed in CF mouse models including increased luminal mucus accumulation and goblet cell hyperplasia (see Fig. 5).

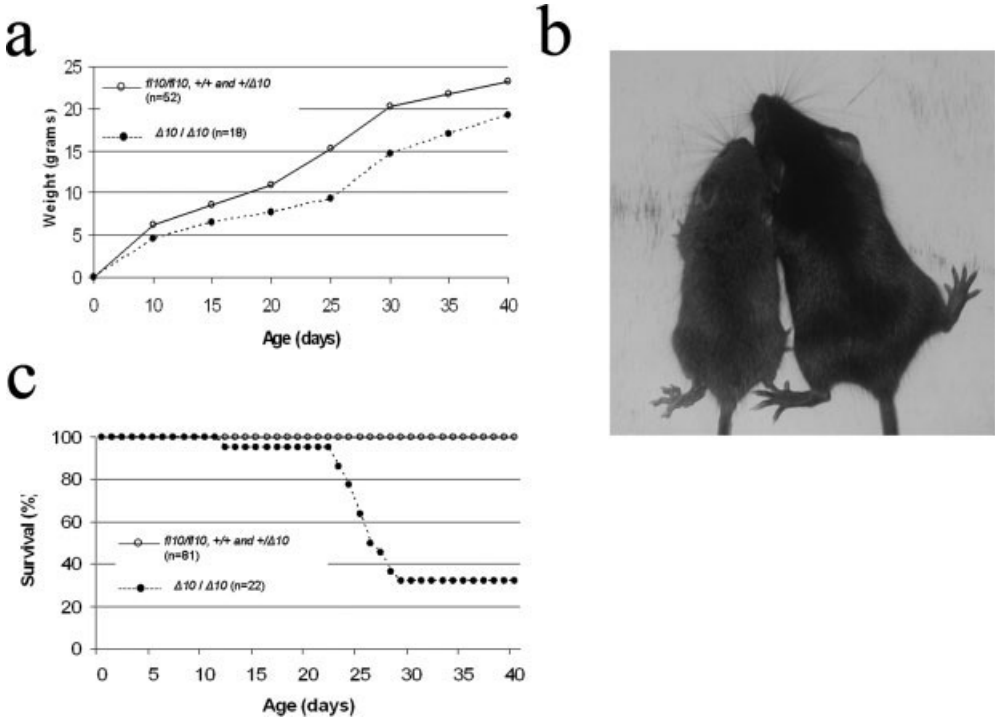

FIG. 4. Phenotype of *Cftr*−/− mice created from the conditional null allele. (**a**) Growth curve for $Cftr^{fl10/fl10}$, $Cftr^{+/+}$, $Cftr^{+/\Delta 10}$, and $Cftr^{\Delta 10/\Delta 10}$ mice. (**b**) Representative picture of $Cftr^{\Delta 10/\Delta 10}$ (left) and $Cftr^{+/+}$ (right) littermates (20 days old). (**c**) Survival curve for $Cftr^{fl10/fl10}$, $Cftr^{+/+}$, $Cftr^{+/\Delta 10}$, and $Cftr^{\Delta 10/\Delta 10}$ mice. (There was no difference in growth or survival among $Cftr^{fl10/fl10}$, $Cftr^{+/+}$, and $Cftr^{+/\Delta 10}$, so they were combined).

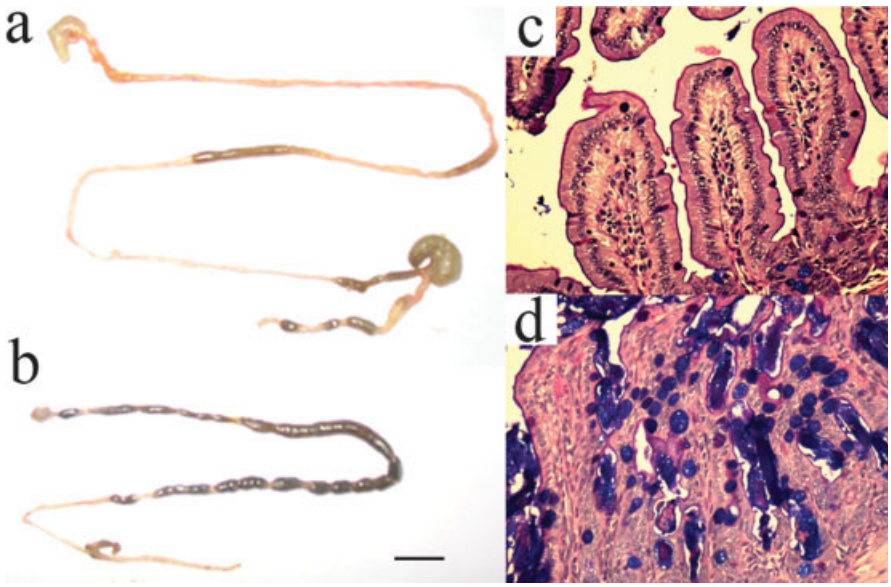

FIG. 5. Characteristics of the intestine from $Cftr^{+/+}$ and $Cftr^{\Delta 10/\Delta 10}$ mice. (**a**) Intestines from $Cftr^{+/+}$ and (**b**) $Cftr^{\Delta 10/\Delta 10}$ mice. $Cftr^{\Delta 10/\Delta 10}$ mice display intestinal blockage (dark areas along intestine) compared with $Cftr^{+/+}$ littermate. Bar is 1 cm. (**c**) Ileum of $Cftr^{+/+}$ and (**d**) $Cftr^{\Delta 10/\Delta 10}$ mice with PAS staining. $Cftr^{+/+}$ ileum displays normal histology whereas $Cftr^{\Delta 10/\Delta 10}$ ileum displays characteristic intestinal disease including goblet cell hyperplasia (purple filled circles), excess luminal mucus and villi fusion. Ileum photomicrographs are ×200 magnification. ($Cftr^{fl10/fl10}$ mice were indistinguishable from $Cftr^{+/+}$ mice).

These results indicate that loss of exon 10 results in a functionally null phenotype in mice, displaying decreased growth, high incidence of intestinal obstruction, goblet cell hyperplasia, and loss of normal transepithelial ion transport. As this allele can be generated in a conditional fashion using the $Cftr^{fl10}$ mouse and regulated Cre expression, it provides a tool to study tissue-specific and temporal effects of losing Cftr. For example, decreased growth and intestinal obstruction in CF mice have been hypothesized to be due to loss of Cftr activity in the intestinal epithelium. This hypothesis can be tested by crossing the $Cftr^{fl10}$ mouse with a mouse in which Cre recombinase expression is driven by the villin promoter so that Cre is expressed specifically in the intestinal epithelium (Madison *et al.*, 2002). Delayed growth in CF mice may also have a neuroendocrine origin given the multiple reports of *Cftr* expression in the brain (Mulberg *et al.*, 1998; Weyler *et al.*, 1999). Possible Cftr function in the nervous system could be examined by crossing the $Cftr^{fl10}$ mouse with a mouse in which Cre expression is driven by the nestin promoter so that Cre is expressed specifically in the central and peripheral nervous system (Tronche *et al.*, 1999). Finally, one can test the importance of Cftr activity on the development of the mouse (e.g., in utero, postnatal, pubertal, and adult) by deleting Cftr function in the whole mouse at different time points by crossing the $Cftr^{fl10}$ mouse with a mouse in which Cre expression is driven by an inducible promoter (e.g., Badea *et al.*, 2003). The ability to delete Cftr in a tissue or time-dependent manner in the mouse will not only help understand how Cftr function contributes to the function and development of each tissue but how the absence of CFTR in these same tissues leads to CF disease in humans.

METHODS AND MATERIALS

Generation of the *Cftr* Floxed Allele

Genomic DNA was isolated from R1 cells. The targeting vector consisted of amplified fragments of *Cftr* that included 4.4 kb of intron 9 (5′ arm), 4.5 kb of intron 10 (3′ arm), and 0.5 kb consisting of exon 10 and ~150 bp of intron 9 and 10 on each side. These fragments were subcloned into pBluescript. Two *loxP* sites surrounding the phosphoglycerol kinase promoter attached to a neomycin-resistance gene (PGK-neocassette) were inserted downstream of exon 10 while the third *loxP* site was inserted upstream of exon 10. A HTK cassette was inserted downstream of intron 10. A schematic of the targeting construct is shown in Figure 1. The linearized targeting vector was transfected into R1 ES cells and neomycin resistant colonies were screened by Southern blot using a 3′ external probe with SphI digested genomic DNA. Three colonies out of 201(1.5%) were correctly targeted. These correctly targeted ES cells were microinjected into C57BL/6 blastocysts and transferred to a pseudopregnant mouse. Eight chimeric males were bred to C57BL/6 females and F1 agouti offspring were analyzed by Southern blot and PCR genotyping to confirm germline transmission of the conditional *Cftr* null allele.

PCR

Genotyping was completed by PCR analysis using DNA extracts from ear biopsies. To detect the $Cftr^{fl10}$ (or $Cftr^{tm1Cwr}$) allele (408 bp), the $Cftr^{+}$ allele (361 bp), and the $Cftr^{\Delta 10}$ allele (154 bp), primers P1 (5′-GTAGGGGCTCGCTCTTCTTT-3′) P2 (5′ GTACCCGGCA-

TAATCCAAGA-3′) and P3 (5′-AGCCCCTCGAGGGACC-TAAT-3′) were used (Fig. 1c,d). PCR reactions were completed for 40 cycles of 95°C for 30 seconds, 58°C for 1 min and 72°C for 1 min.

Lungs and intestines were collected from *Cftr* +/+, +/−, and −/− animals and total RNA was isolated using Trizol (Invitrogen) per the manufacturer's instructions. One μg of RNA was reverse transcribed into cDNA with MMLV. cDNA was used in PCR analysis to amplify *Cftr* exons 8–11 to detect wild-type allele(563 bp) and excised exon 10 allele (371 bp) expression. PCRs were completed for 40 cycles of 95°C for 30 sec, 55°C for 30 sec, and 72°C for 1 min with primers (5′-CCACAGGCA-TAATCATGGAA-3′) and (5′-TGTGACTCCACCTTCTC-CAA-3′).

Histology

Mouse intestines were isolated and fixed in 10% formalin, embedded in paraffin and sectioned every 5 μm. Periodic acid schiff (PAS) staining of these sections were completed to detect mucus accumulation.

Bioelectric Measurements

The potential difference (PD) across the nasal epithelium of the mice was measured according to procedures previously described elsewhere (Brady *et al*., 2001; Kelley *et al*., 1997), with some modifications. Mice were anesthetized with 8.5 mg/ml ketamine, 1.7 mg/ml xylazine, and 0.3 mg/ml acepromazine in sterile saline. Animals were dosed intraperitoneally with 0.012 ml/g mouse weight. A PE-10 tube stretched to one-half the original diameter was inserted 2 mm into the mouse nostril and placed against the septum. With the use of a syringe pump (model A-99; Razel Scientific Instruments) and 3-ml syringes, *N*-2-hydroxyethylpiperazine-*N*′-2-ethanesulfonic acid (HEPES)-buffered Ringer's solution perfused into the nostril at a rate of 5 ml/min. Valves controlled the solution which entered the nostril, with a 15-sec delay until the new solution reached the nasal epithelium. Readings were taken until a steady-state value was reached before perfusing the nasal epithelium with a new solution. Paper wicks were used to absorb excess liquid from the mouth and opposite nostril of the mouse being tested. A trachea tube consisting of an Angiocath IV Catheter was inserted into the mouse trachea to facilitate breathing. Bridges (4% agar) connected the tubing to calomel electrodes, and each bridge was made in the same solution as the perfusate it measured (HEPES-buffered Ringer's or chloridefree HEPES-buffered Ringer's). A needle containing 4% agar in HEPES-buffered Ringer's was placed subcutaneously in the mouse's back and connected to another calomel electrode to serve as a reference. The measuring and reference calomel electrodes were situated in a KCl bath in which one end of the agar bridge was also immersed. The other end of the measuring electrode's bridge was in contact with the perfusate 20 cm from the mouse nose. The transepithelial difference was measured with a voltmeter (model ISO-DAM-D; World Precision Instruments), and the signal was recorded on a chart recorder (model BD112; Kipp and Zonen). The PD measurements were corrected for junction potentials, and changes in PD values were calculated by subtracting the value after 4 min of perfusion with chloride-free Ringer's solution containing forskolin from the value when the perfusion began. Before measurements, the system was zeroed by adjusting the voltmeter after connecting the reference needle to the tube normally placed in the mouse nose to complete the circuit.

Electrolyte transport was investigated in the intestine of 8- to 12-week-old animals that were fasted overnight. Mice were rendered unconscious by CO_2 asphyxiation and killed by exsanguination. The large and small intestines were removed and immediately placed in ice-cold HEPES-buffered Ringer's solution (in mM: 138 NaCl, 5 KCl, 2.5 Na_2HPO_4, 1.8 $CaCl_2$, 1.0 $MgSO_4$, and 10 HEPES-NaOH, pH 7.4) for dissection. The intestine was cut longitudinally, and the contents were removed with a stream of Ringer's solution. The tissue was stretched and pinned in an Ussing chamber with an aperture of 0.125 cm^2. Tissues were bathed on both sides by 6–8 ml of mammalian Krebs-Ringer bicarbonate solution [in mM: 115 NaCl, 25 $NaHCO_3$, 5 KCl, 2.5 Na_2HPO_4, 1.8 $CaCl_2$, 1.0 $MgSO_4$, and 10 glucose, pH 7.4 (mannitol replaced glucose in the apical bathing solution)], which was warmed to 37°C and circulated with 95% O_2–5% CO_2 through gas lifts. Transepithelial electrical voltage difference (V_{ms}) was measured between two Ringer–agar bridges. Calomel cells connected the bridges to a high-impedance voltmeter (DVC 1,000 Voltage/Current Clamp, World Precision Instruments). Current from an external DC source was passed by silver–silver chloride electrodes and Ringer–agar bridges to clamp the spontaneous V_{ms} to zero. The current required (short-circuit current, I_{sc}) was corrected for solution resistance between the tips of the voltage-sensing electrodes and recorded. Tissues were maintained with V_{ms} clamped to zero (short-circuit conditions). At 60-sec intervals, V_{ms} was clamped to +2 mV for 3 sec to calculate transepithelial resistance (R_{ms}). Tissues were mounted and observed until the I_{sc} stabilized (generally 10–15 min), at which time experimental maneuvers were begun.

ACKNOWLEDGMENTS

The authors thank Nicole Brown and Christine Zhang for their assistance with the bioelectric measurements and Bill Marcus for assistance with genotyping.

LITERATURE CITED

Badea TC, Wang Y, Nathans J. 2003. A noninvasive genetic/pharmacologic strategy for visualizing cell morphology and clonal relationships in the mouse. J Neurosci 23:2314–2322.

Ben-Chetrit A, Antenos M, Jurisicova A, Pasyk EA, Chitayat D, Foskett JK, Casper RF. 2002. Expression of cystic fibrosis transmembrane conductance regulator during early human embryo development. Mol Hum Reprod 8:758–764.

Brady KG, Kelley TJ, Drumm ML. 2001. Examining basal chloride transport using the nasal potential difference response in a murine model. Am J Physiol Lung Cell Mol Physiol 281:L1173–L1179.

Colledge WH, Abella BS, Southern KW, Ratcliff R, Jiang C, Cheng SH, MacVinish LJ, Anderson JR, Cuthbert AW, Evans MJ. 1995. Generation and characterization of a delta F508 cystic fibrosis mouse model. Nat Genet 10:445–452.

Davies WL, Vandenberg JI, Sayeed RA, Trezise AE. 2004. Cardiac expression of the cystic fibrosis transmembrane conductance regulator involves novel exon 1 usage to produce a unique amino-terminal protein. J Biol Chem 279:15877–15887.

Delaney SJ, Alton EW, Smith SN, Lunn DP, Farley R, Lovelock PK, Thomson SA, Hume DA, Lamb D, Porteous DJ, Dorin JR, Wainwright BJ. 1996. Cystic fibrosis mice carrying the missense mutation G551D replicate human genotype-phenotype correlations. Embo J 15: 955–963.

Devuyst O, Golstein PE, Sanches MV, Piontek K, Wilson PD, Guggino WB, Dumont JE, Beauwens R. 1997. Expression of CFTR in human and bovine thyroid epithelium. Am J Physiol 272:C1299–C1308.

Engelhardt JF, Yankaskas JR, Ernst SA, Yang Y, Marino CR, Boucher RC, Cohn JA, Wilson JM. 1992. Submucosal glands are the predominant site of CFTR expression in the human bronchus. Nat Genet 2:240–248.

Gadsby DC, Vergani P, Csanady L. 2006. The ABC protein turned chloride channel whose failure causes cystic fibrosis. Nature 440:477–483.

Grubb BR, Boucher RC. 1999. Pathophysiology of gene-targeted mouse models for cystic fibrosis. Physiol Rev 79:S193–S214.

Hasty P, O'Neal WK, Liu KQ, Morris AP, Bebok Z, Shumyatsky GB, Jilling T, Sorscher EJ, Bradley A, Beaudet AL. 1995. Severe phenotype in mice with termination mutation in exon 2 of cystic fibrosis gene. Somat Cell Mol Genet 21:177–187.

Hodges CA, Palmert MR, Drumm ML. 2008. Infertility in females with cystic fibrosis is multifactorial: Evidence from mouse models. Endocrinology 149:2790–2797.

Jin R, Hodges CA, Drumm ML, Palmert MR. 2006. The cystic fibrosis transmembrane conductance regulator (Cftr) modulates the timing of puberty in mice. J Med Genet 43:e29, 1–4.

Kartner N, Augustinas O, Jensen TJ, Naismith AL, Riordan JR. 1992. Mislocalization of delta F508 CFTR in cystic fibrosis sweat gland. Nat Genet 1:321–327.

Kelley TJ, Thomas K, Milgram LJ, Drumm ML. 1997. In vivo activation of the cystic fibrosis transmembrane conductance regulator mutant deltaF508 in murine nasal epithelium. Proc Natl Acad Sci USA 94:2604–2608.

Kent G, Oliver M, Foskett JK, Frndova H, Durie P, Forstner J, Forstner GG, Riordan JR, Percy D, Buchwald M. 1996. Phenotypic abnormalities in long-term surviving cystic fibrosis mice. Pediatr Res 40:233–241.

Madison BB, Dunbar L, Qiao XT, Braunstein K, Braunstein E, Gumucio DL. 2002. Cis elements of the villin gene control expression in restricted domains of the vertical (crypt) and horizontal (duodenum, cecum) axes of the intestine. J Biol Chem 277:33275–33283.

Manson AL, Trezise AE, MacVinish LJ, Kasschau KD, Birchall N, Episkopou V, Vassaux G, Evans MJ, Colledge WH, Cuthbert AW, Huxley C. 1997. Complementation of null CF mice with a human CFTR YAC transgene. EMBO J 16:4238–4249.

Mulberg AE, Weyler RT, Altschuler SM, Hyde TM. 1998. Cystic fibrosis transmembrane conductance regulator expression in human hypothalamus. Neuroreport 9:141–144.

O'Gorman S, Dagenais NA, Qian M, Marchuk Y. 1997. Protamine-Cre recombinase transgenes efficiently recombine target sequences in the male germ line of mice, but not in embryonic stem cells. Proc Natl Acad Sci USA 94:14602–14607.

O'Neal WK, Hasty P, McCray PB Jr, Casey B, Rivera-Perez J, Welsh MJ, Beaudet AL, Bradley A. 1993. A severe phenotype in mice with a duplication of exon 3 in the cystic fibrosis locus. Hum Mol Genet 2:1561–1569.

Ratcliff R, Evans MJ, Cuthbert AW, MacVinish LJ, Foster D, Anderson JR, Colledge WH. 1993. Production of a severe cystic fibrosis mutation in mice by gene targeting. Nat Genet 4:35–41.

Robert R, Thoreau V, Norez C, Cantereau A, Kitzis A, Mettey Y, Rogier C, Becq F. 2004. Regulation of the cystic fibrosis transmembrane conductance regulator channel by beta-adrenergic agonists and vasoactive intestinal peptide in rat smooth muscle cells and its role in vasorelaxation. J Biol Chem 279:21160–21168.

Rozmahel R, Wilschanski M, Matin A, Plyte S, Oliver M, Auerbach W, Moore A, Forstner J, Durie P, Nadeau J, Bear C, Tsui LC. 1996. Modulation of disease severity in cystic fibrosis transmembrane conductance regulator deficient mice by a secondary genetic factor. Nat Genet 12:280–287.

Snouwaert JN, Brigman KK, Latour AM, Malouf NN, Boucher RC, Smithies O, Koller BH. 1992. An animal model for cystic fibrosis made by gene targeting. Science 257:1083–1088.

Todd-Turla KM, Rusvai E, Naray-Fejes-Toth A, Fejes-Toth G. 1996. CFTR expression in cortical collecting duct cells. Am J Physiol 270:F237–F244.

Trezise AE, Buchwald M. 1991. In vivo cell-specific expression of the cystic fibrosis transmembrane conductance regulator. Nature 353:434–437.

Trezise AE, Chambers JA, Wardle CJ, Gould S, Harris A. 1993a. Expression of the cystic fibrosis gene in human foetal tissues. Hum Mol Genet 2:213–218.

Trezise AE, Linder CC, Grieger D, Thompson EW, Meunier H, Griswold MD, Buchwald M. 1993b. CFTR expression is regulated during both the cycle of the seminiferous epithelium and the oestrous cycle of rodents. Nat Genet 3:157–164.

Tronche F, Kellendonk C, Kretz O, Gass P, Anlag K, Orban PC, Bock R, Klein R, Schutz G. 1999. Disruption of the glucocorticoid receptor gene in the nervous system results in reduced anxiety. Nat Genet 23:99–103.

Tsui LC. 1992. The spectrum of cystic fibrosis mutations. Trends Genet 8:392–398.

Weyler RT, Yurko-Mauro KA, Rubenstein R, Kollen WJ, Reenstra W, Altschuler SM, Egan M, Mulberg AE. 1999 CFTR is functionally active in GnRH-expressing GT1–7 hypothalamic neurons. Am J Physiol 277:C563–C571.

Yang Y, Raper SE, Cohn JA, Engelhardt JF, Wilson JM. 1993. An approach for treating the hepatobiliary disease of cystic fibrosis by somatic gene transfer. Proc Natl Acad Sci USA 90:4601–4605.

Yoshimura K, Nakamura H, Trapnell BC, Chu CS, Dalemans W, Pavirani A, Lecocq JP, Crystal RG. 1991. Expression of the cystic fibrosis transmembrane conductance regulator gene in cells of non-epithelial origin. Nucleic Acids Res 19:5417–5423.

Zeiher BG, Eichwald E, Zabner J, Smith JJ, Puga AP, McCray PB Jr, Capecchi MR, Welsh MJ, Thomas KR. 1995. A mouse model for the delta F508 allele of cystic fibrosis. J Clin Invest 96:2051–2064.